AGU PUBLICATIONS

Geophysical Research Letters

RESEARCH LETTER
10.1002/2014GL062040

Key Points:
- Vertical mixing introduces significant errors in O_2/Ar-NCP estimates
- Model results show that a composite N_2O-O_2/Ar tracer improves NCP estimates

Supporting Information:
- Readme
- Text S1
- Figure S1

Correspondence to:
N. Cassar,
Nicolas.Cassar@Duke.edu

Citation:
Cassar, N., C. D. Nevison, and M. Manizza (2014), Correcting oceanic O_2/Ar-net community production estimates for vertical mixing using N_2O observations, *Geophys. Res. Lett.*, *41*, 8961–8970, doi:10.1002/2014GL062040.

Received 30 SEP 2014
Accepted 6 NOV 2014
Accepted article online 10 NOV 2014
Published online 18 DEC 2014

Correcting oceanic O_2/Ar-net community production estimates for vertical mixing using N_2O observations

Nicolas Cassar[1], Cynthia D. Nevison[2], and Manfredi Manizza[3]

[1]Division of Earth and Ocean Sciences, Nicholas School of the Environment, Duke University, Durham, North Carolina, USA, [2]INSTAAR, University of Colorado at Boulder, Boulder, Colorado, USA, [3]Geosciences Research Division, Scripps Institution of Oceanography, University of California, San Diego, California, USA

Abstract The O_2/Ar approach has become a key method to estimate oceanic net community production (NCP). However, in some seasons and regions of the ocean, strong vertical mixing of O_2-depleted deepwater introduces a large error into O_2/Ar-derived NCP estimates. In these cases, undersaturated-O_2/Ar observations have for all intents and purposes been ignored. We propose to combine underway O_2/Ar and N_2O observations into a composite tracer that is conservative with respect to the influence of vertical mixing on the surface biological O_2 inventory. We test the proposed method with an ocean observing system simulation experiment (OSSE) in which we compare N_2O-O_2/Ar and O_2/Ar-only gas flux estimates of NCP to the model-simulated true NCP in the Southern Ocean. Our proof-of-concept simulations show that the N_2O-O_2/Ar tracer significantly improves NCP estimates when/where vertical mixing is important.

1. Introduction: Uncertainties in O_2/Ar-NCP

Oxygen (O_2) and argon (Ar) have similar solubility properties. Whereas O_2 concentration at the ocean surface is influenced by physical and biological processes, Ar is biologically inert. Measurements of the O_2/Ar elemental ratio can therefore be used to assess the influence of biological processes on the O_2 concentration [*Craig and Hayward*, 1987]. Mainly, O_2/Ar reflects the balance between photosynthesis and respiration, i.e., net community production (NCP). The O_2/Ar approach is increasingly being adopted by various groups [*Cassar et al.*, 2011; *Hamme et al.*, 2012; *Huang et al.*, 2012; *Palevsky et al.*, 2013; *Reuer et al.*, 2007; *Spitzer and Jenkins*, 1989; *Stanley et al.*, 2010], with new methods allowing for high-resolution measurements [e.g., *Cassar et al.*, 2009; *Tortell*, 2005]. However, the O_2/Ar-NCP approach harbors limitations and uncertainties, some of which are described below.

Using the O_2/Ar approach, NCP generally is approximated as follows:

$$NCP\left(mmol\ C\ m^{-2}d^{-1}\right) \approx k_{O_2} {}^{*} O_{2sat} {}^{*} \Delta(O_2/Ar) {}^{*} r_{C:O2} \tag{1}$$

where k_{O_2} and O_{2sat} are the O_2 piston velocity and saturation concentration, respectively. $r_{C:O2}$ is the molar photosynthetic quotient for NCP. The biological O_2 supersaturation, $\Delta(O_2/Ar)$, is defined as:

$$\Delta(O_2/Ar) = \left[\frac{(O_2/Ar)}{(O_2/Ar)_{sat}} - 1\right] \tag{2}$$

In equation (1), it is assumed that the argon is at saturation. In reality, the argon saturation commonly deviates from saturation by a couple of percent in the open ocean and more in ice-covered regions, introducing an error of this magnitude in the NCP estimates. In addition, the uncertainty in $r_{C:O2}$, which is generally assumed to be constant at about 1:1.4 mol C: mol O_2, is thought to be on the order of 10% or less [*Laws* [1991]. Overall, these two sources of error are likely small under most conditions compared to the errors discussed below.

The gas exchange velocity k_{O_2} must be estimated in order to convert the biological O_2 supersaturation to NCP. k_{O_2} is generally estimated using a wind speed gas exchange parameterization [*Reuer et al.*, 2007; *Wanninkhof*, 1992], with an uncertainty of approximately ±30% [e.g., *Bender et al.*, 2011]. Several methods, including upper ocean radon distribution, have been used to assess and potentially reduce this uncertainty [*Bender et al.*, 2011; *Peng et al.*, 1979; *van der Loeff et al.*, 2014].

Intrinsic in the calculation above are the assumptions that mixed layer depth and NCP are constant over the residence time of O_2 at the ocean surface, and that the biological oxygen pool is homogeneous and at steady state in the mixed layer. The errors associated with these assumptions have recently been assessed through modeling and Lagrangian observations, where the time rate of change of the biological O_2 inventory was measured [*Hamme et al*., 2012; *Jonsson et al*., 2013; *Martin et al*., 2013]. In order to estimate carbon export production, the organic carbon pool must also be at steady state. The degree to which this is the case varies but is only relevant if NCP is used to infer carbon export production.

An additional source of uncertainty, and the subject of this study, is associated with the assumption of no vertical mixing of O_2. $\Delta(O_2/Ar)$ at the ocean surface is a function of NCP-derived O_2 and a vertical mixing component. We hereafter loosely use the term vertical mixing to refer to all obduction processes including upwelling, entrainment, and diapycnal mixing such as lateral induction (i.e., horizontal flow across the sloping base of the mixed layer). Using a prognostic model, *Jonsson et al*. [2013] have shown that vertical fluxes at the base of the mixed layer can introduce significant errors in the estimate of NCP. These model results are supported by field observations that suggest that the O_2 budget at the ocean surface can be dominated by vertical mixing processes [*Castro-Morales et al*., 2013; *Giesbrecht et al*., 2012; *Weeding and Trull*, 2014]. In some regions and during some periods of the year, vertical mixing is likely the largest source of error in O_2/Ar-NCP estimates. The difficulty in assessing the effective vertical diffusivity coefficients and large uncertainties (factor of 10 or more) in such estimates over the residence time of O_2 at the ocean surface generally preclude any meaningful correction, even when the vertical gradients in O_2/Ar are well constrained. Because of these uncertainties and our current inability to account for vertical mixing, negative $\Delta(O_2/Ar)$ measurements are in large part currently ignored [*Cassar et al*., 2007; *Giesbrecht et al*., 2012; *Reuer et al*., 2007]. In the process of systematically discarding negative $\Delta(O_2/Ar)$, however, we are missing the opportunity to improve our very limited understanding of processes associated with surface heterotrophy [see *Duarte et al*., 2013; *Ducklow and Doney*, 2013; *Williams et al*., 2013]. Furthermore, it also seems likely that autotrophic regions (positive $\Delta(O_2/Ar)$) are impacted to various degrees by vertical mixing and that the O_2/Ar approach may be underestimating NCP in regions where vertical mixing of O_2 depleted waters is important..

Below, we present an approach to correct O_2/Ar-NCP for vertical mixing using surface nitrous oxide (N_2O). The method decomposes the biological O_2 signal into a vertical mixing and autochthonous surface signal, thereby correcting the O_2/Ar-NCP estimates. As importantly, the method can be used to identify regions or episodes of surface heterotrophy because the latter does not impact the N_2O signal (cf. see below).

2. Background: Oceanic Distribution of N_2O and Relation to O_2

As a potent greenhouse gas and contributor to stratospheric ozone depletion, N_2O plays an important role in Earth's climate. The oceans are believed to contribute approximately one third of the natural N_2O flux to the atmosphere [*Hirsch et al*., 2006; *Seitzinger et al*., 2000]. Oceanic sources of N_2O are only poorly constrained based on bottom up estimates, with a range of 1.2–6.8 Tg N yr^{-1} [*Nevison et al*., 1995, 2003] but generally fall in a narrower 4–6 Tg N yr^{-1} range in recent top down atmospheric inversions [*Saikawa et al*., 2014; *Thompson et al*., 2014].

In the oceans, N_2O is produced as a by-product of biological decomposition of organic matter at depth [*Cohen and Gordon*, 1978; *Elkins et al*., 1978; *Yoshinari*, 1976]. In regions where O_2 availability is sufficient, N_2O is produced mainly as a result of nitrification. Because nitrification conventionally has been thought to be photoinhibited [*Horrigan et al*., 1981] [although recent studies have challenged this conventional viewpoint, e.g., *Smith et al*., 2014], most N_2O production occurs below the euphotic zone. Vertical mixing of this N_2O produced at depth, at a rate faster than atmospheric equilibration, leads to N_2O supersaturation at the ocean surface [*Lueker et al*., 2003; *Rees et al*., 1997; *Rhee et al*., 2009].

An inverse relationship between N_2O and O_2 at depth was first reported by *Yoshinari* [1976]. Since Yoshinari's seminal study, a linear stoichiometry between N_2O and the AOU of approximately ~0.1 mmol N_2O/mol O_2 has been observed in numerous oceanic regions [*Bange and Andreae*, 1999; *Cohen and Gordon*, 1979; *Elkins et al*., 1978; *Law and Owens*, 1990; *Nevison et al*., 2003; *Oudot et al*., 1990; *Rees et al*., 1997; *Walter et al*., 2006], where AOU is the Apparent O_2 Utilization (AOU) and is defined as $O_{2_{sat}} - O_{2_{measured}}$, and reflects remineralization at depth.

The linearity of the relationship between N_2O and AOU has been used as a basis for modeling N_2O production as a function of oxygen consumption in ocean biogeochemistry models [*Suntharalingam and Sarmiento*, 2000]. In addition, the N_2O/AOU stoichiometric relationship has been exploited by *Nevison et al.* [2012, 2005] to estimate the seasonal signature of ventilation in atmospheric potential oxygen (APO), thus allowing the NCP signal to be calculated as a residual of known terms. This approach assumes that the seasonal cycle in APO is the net result of contributions from oceanic NCP, thermal variations, and ventilation. APO, estimated as APO ~ $\delta O_2/N_2 + 1.1\ CO_2$, corrects for the influence of terrestrial photosynthesis and respiration [*Stephens et al.*, 1998].

3. Discussion: Proposed N_2O-O_2/Ar NCP Approach

3.1. Description of N_2O-O_2/Ar Composite Tracer

In this proof-of-concept study, we explore the use of underway high resolution measurements of dissolved N_2O in parallel with regular O_2/Ar and N_2O depth profiles, to constrain the relative proportion of surface and vertically mixed biological O_2. This is analogous to the approach of *Nevison et al.* [2005, 2012], as discussed above, in correcting for ventilation influences to isolate the contribution of NCP to APO. This method is particularly timely considering the recent development of methods for underway N_2O by spectroscopy [*Arévalo-Martínez et al.*, 2013; *Grefe and Kaiser*, 2013]. The analytical error of less than 0.1% in these N_2O measurements is well below the uncertainties associated with the wind parameterization of the gas exchange coefficients. The recent commercialization of laser-based isotopic N_2O analyzers could also provide further constraints on the N_2O production pathways and origins.

At the ocean surface, the biological oxygen inventory is a function of NCP, loss to the atmosphere, and vertical mixing of biological O_2 (O_{2_B}) to the surface:

$$MLD\frac{dO_{2_{B\,MLD}}}{dt} = NCP - k_z\frac{\partial O_{2_B}}{\partial z} - k_{O2}O_{2_{B\,MLD}} \tag{3}$$

where k_z is the apparent vertical mixing coefficient ($m^2\,s^{-1}$), which includes all obduction terms (upwelling, lateral induction, entrainment, diffusion, etc.). *MLD* and k_{O2} are the mixed-layer depth and O_2 piston velocity, respectively. The total O_2 ($O_{2_{total}}$) is equal to the sum of O_2 at saturation, O_2 associated with physical processes (O_{2P}), and O_2 derived from biological processes (O_{2B}). O_{2_B} is equal to ($O_{2_{sat}}\Delta(O_2/Ar)$) (assuming Ar at saturation; see introduction). Similarly, biological N_2O at the surface (where $(N_2O)_B = (N_2O)_{Total} - (N_2O)_{Thermal}) - (N_2O)_{sat}$ is a function of vertical mixing and gas exchange with the atmosphere. Because nitrification is photoinhibited, there are no significant sources of N_2O in the surface (cf. see section on caveats and limitations below):

$$MLD\frac{d(N_2O)_{B_{MLD}}}{dt} = -k_z\frac{\partial(N_2O)_B}{\partial z} - k_{N2O}(N_2O)_{B_{MLD}} \tag{4}$$

Similar to the $\Delta(O_2/Ar)$ nomenclature, $(N_2O)_B = ([N_2O]_{sat}\Delta(N_2O)_B)$, where $\Delta(N_2O)_B$ is the biological N_2O supersaturation. Multiplying equation (4) by the stoichiometric ratio of vertical gradients $\frac{\partial O_{2_B}}{\partial(N_2O)_B}$, and subtracting it from equation (3) and rearranging:

$$MLD\left[\frac{d}{dt}\left(O_{2_{B\,MLD}} - \frac{\partial O_{2_B}}{\partial(N_2O)_B}(N_2O)_{B_{MLD}}\right)\right] = NCP - k_{O2}O_{2_{B\,MLD}} + \frac{\partial O_{2_B}}{\partial(N_2O)_B}k_{N2O}(N_2O)_{B_{MLD}} \tag{5}$$

Assuming steady state and neglecting Ar deviation from saturation, NCP can be approximated as:

$$NCP\left(mmol\ O_2\ m^{-2}d^{-1}\right) = k_{O2}\left[[O_2]_{sat}\Delta\left(\frac{O_2}{Ar}\right) - \frac{k_{N2O}}{k_{O2}}\frac{\partial O_{2_B}}{\partial(N_2O)_B}(N_2O)_{B_{MLD}}\right] \tag{6}$$

Based on the equations in *Wanninkhof* [1992], the O_2/N_2O piston velocity ratio $\frac{k_{N2O}}{k_{O2}}$ is ~0.92 and independent of wind speed with negligible dependence on temperature (Figure 1 upper panel). The ratio of surface-to-subsurface gradient in biological O_2 and N_2O concentrations $\frac{\partial O_{2_B}}{\partial(N_2O)_B}$ can be estimated from $\frac{\left(O_{2_{B\,MLD}} - O_{2_{B\,deep}}\right)}{\left((N_2O)_{B_{MLD}} - (N_2O)_{B\,deep}\right)}$ where

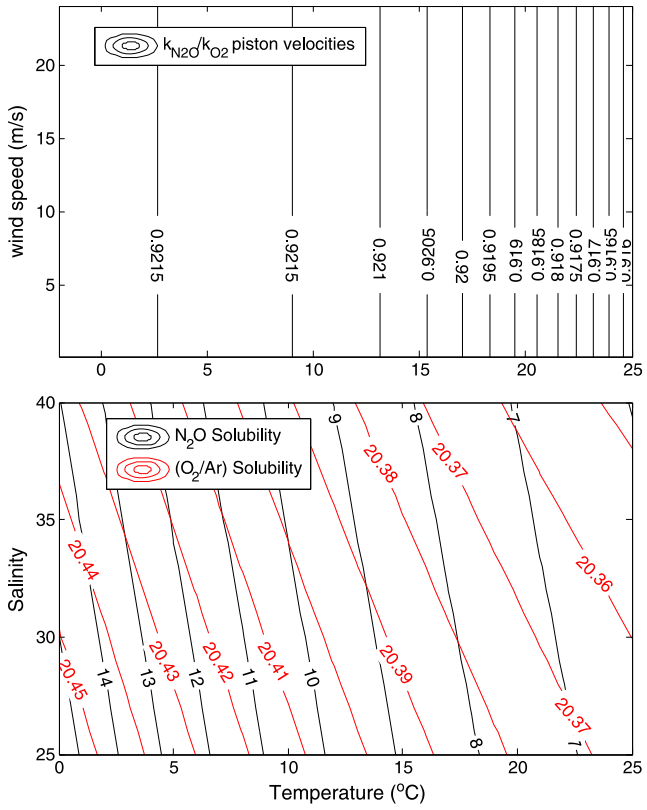

Figure 1. Comparison of O_2 and N_2O piston velocity (top panel) and solubility properties (bottom panel). Isopleths of N_2O and O_2/Ar solubilities are in nmol kg^{-1} and unitless, respectively.

deepend-members are measured at a given depth below the mixed layer. If depth profiles of O_2/Ar are not available, the deep end-member of the biological oxygen concentration can be approximated with AOU, since vertical gradients in Ar saturation are generally small [*Hamme and Severinghaus*, 2007]. Equation (6) can of course be expanded to account for the non-steady state conditions and Ar deviation from saturation. Finally, we note that the N_2O correction shown in equation (6) may also be applicable to other tracers. For example, it may be applied to gross primary production (GPP) estimates based on the triple O_2 isotope composition of dissolved O_2 in the oceans. *Nicholson et al.* [2014] recently showed with model sim ulations that vertical mixing is often the largest source of bias in triple-O_2-isotope estimates of GPP.

With simple algebraic manipulations, it can be shown that NCP also can be described in terms of the flux of the individual gases as follows:

$$NCP = k_{O2}\left(O_{2_{MLD}} - O_{2_{sat}}\right) - \frac{O_{2_{sat}}}{\mathrm{Ar}_{sat}} k_{Ar}\left(\mathrm{Ar}_{MLD} - \mathrm{Ar}_{sat}\right) - \frac{\partial O_{2_B}}{\partial (N_2O)_B} k_{N2O}(N_2O)_{B_{MLD}} \quad (7)$$

where the first, second, and third terms on the right-hand side represent O_2, Ar, and biological N_2O fluxes at the ocean surface, respectively. The second and third terms are corrected for the elemental stoichiometries of Ar and N_2O, respectively, relative to O_2. The total O_2 flux is equal to the sum of biological and physical O_2 fluxes. The biological O_2 flux is therefore equal to the total O_2 flux (first term) minus the Ar flux corrected for the O_2/Ar stoichiometry (second term). The biological N_2O flux at the ocean surface (third term) removes the influence of vertical mixing on the biological O_2 flux.

3.2. Observing System Simulation Experiment (OSSE): Model Description and Results

To assess the influence of including N_2O observations on estimates of NCP, we use a model-based ocean Observing System Simulation Experiment (OSSE) focusing on the Southern Ocean, which is a region where vertical mixing can be significant and thus is particularly well suited for our approach. Earlier estimates hypothesized the Southern Ocean to be a large source of N_2O to the atmosphere, with the latitude band between 30°S and 90°S contributing 35–45% of total oceanic N_2O emissions [*Nevison et al.*, 1995; *Suntharalingam and Sarmiento*, 2000]. More recent estimates fall in the range of ~10% of open ocean emissions [*Hirsch et al.*, 2006; *Nevison et al.*, 2012]. Upwelling is especially important south of the polar front, where strong winds lead to Ekman pumping and ventilation of deep waters. *Rees et al.* [1997] found that an increase in dissolved N_2O poleward was consistent with upwelling of N_2O rich waters. More recently, *Boontanon et al.* [2010] presented observations that "strongly suggest that N_2O production and consumption are related to apparent oxygen utilization" in the Southern Ocean.

In the OSSE presented here, model simulations of NCP are treated as truth. The NCP estimates based on N_2O-O_2/Ar and O_2/Ar-only gas fluxes are compared to the model simulated (i.e., "true") NCP to assess the improvement associated with incorporation of N_2O observations. For this study, we used the Massachusetts

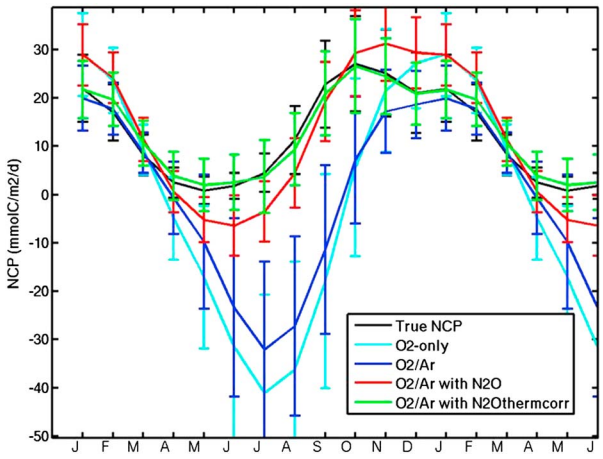

Figure 2. Climatological monthly mean seasonal cycle in true and estimated net community production (NCP) integrated over all model grid points in the region between 41°S and 60°S. Error bars represent the standard deviation of all integrated grid points for each month. The blue curve is based on equation (1). The red curve is based on equation (7), where the $(N_2O)_{B_{MLD}}$ is replaced by the total N_2O concentration in the mixed layer. The green curve is based on equation (10), where $\frac{\partial O_{2_B}}{\partial (N_2O)_B}$ is replaced by $\frac{\partial O_{2_B}}{\partial (N_2O)}$.

Institute of Technology (MIT) general circulation model [MITgcm, *Marshall et al*., 1997] with a coarse horizontal configuration (2.8° by 2.8°) and 15 vertical levels whose first uppermost boxes are 50 and 70 m thick, respectively. The model implements a time step of 15 min for ocean physics and 12 h for ocean biogeochemistry. The physical framework has a northern limit set at 80°N so the Arctic Ocean is only partially represented. Due to the coarse horizontal resolution, the effect of eddy-induced mixing is parameterized according to *Gent and McWilliams* [1990]. The physical model is forced by climatological fluxes of heat [*Jiang et al*., 1999] and wind speed [*Trenberth et al*., 1989] repeated in each simulated year. A climatological sea-ice coverage is applied as described by *Dutkiewicz et al*. [2005]. The biogeochemical model used for this study builds on the work of *Dutkiewicz et al*. [2005] and has an explicit ecosystem module based on two phytoplankton groups (diatoms and non-diatoms) and one generic zooplankton grazing group. The standard MITgcm fully represents the marine O_2 cycle and was expanded by *Manizza et al*. [2012] to include a marine cycle of N_2O, Ar, and some "ad hoc" O_2-like tracers. The latter allow the separation of processes affecting the seasonal cycle of oceanic O_2, including thermal solubility, NCP, and physical ventilation. Additionally, the model carries a N_2O-like tracer (so-called "N_2O thermal") that accounts for the solubility effect on the N_2O cycle. Subtracting this thermal component from total N_2O allows for the isolation of the biological or ventilation-driven component of the N_2O cycle. A more detailed description of the biogeochemical tracer decomposition applied to the O_2 and N_2O cycles and air-sea gas exchange parameterization can be found in *Manizza et al*. [2012].

The MITgcm model used in our study includes a number of limitations. First, it does not represent eddies, even though they can make an important contribution to fine-scale structure and the large-scale mass balance. Furthermore, current ocean biogeochemical models, including MITgcm, generally have significant biases in estimates of the phase and amplitude of the seasonal cycle of CO_2 in the Southern Ocean, which may in part be attributed to a poor representation of seasonality in vertical mixing and mixed-layer depth dynamics [*Lenton et al*., 2013; *Rodgers et al*., 2014]. Despite these limitations and the likelihood that our predictions are model dependent, we note that the objective with the current OSSE is not to test the MITgcm's representation of NCP or its seasonal cycle, but to compare the model's simulated true NCP with the one predicted based on gas fluxes at the ocean surface.

The OSSE shows that including N_2O, and especially $(N_2O)_{B_{MLD}}$ in the equations above, significantly improves the estimates of NCP when and where vertical mixing is important. Overall, the seasonal cycle in NCP is best reproduced with $O_2/\mathrm{Ar} - (N_2O)_{B_{MLD}}$ gas fluxes (equation (5)), closely followed by estimates based on O_2/Ar-N_2O. As expected, O_2-only and O_2/Ar fluxes do poorly during months when vertical mixing is important (Figure 2). Most field measurements of NCP are, however, performed during the growing season, because NCP is expected to be small during the winter's months (Figure 2). Most current in situ observations have been collected in the summer months when O_2/Ar-NCP estimates are relatively accurate. However, our results show that vertical mixing can lead to a negative bias in the O_2/Ar-NCP estimates even during the growing season, and that this bias is for the most part removed when including the N_2O tracer (Figure 3). The improvement is most significant during the early part of the growing season (October–November) when vertical mixing is substantial (Figures 4 and 5). In the case of O_2/Ar-NCP, almost 50% of the estimates are negatively biased by 10 mmol C m^{-2} d^{-1} or more. Including the $(N_2O)_{B_{MLD}}$ tracer leads to almost 70% of the observations being within a few mmol C m^{-2} d^{-1} from the true NCP, and almost 95% within less than 10 mmol C m^{-2} d^{-1} (Figure 4).

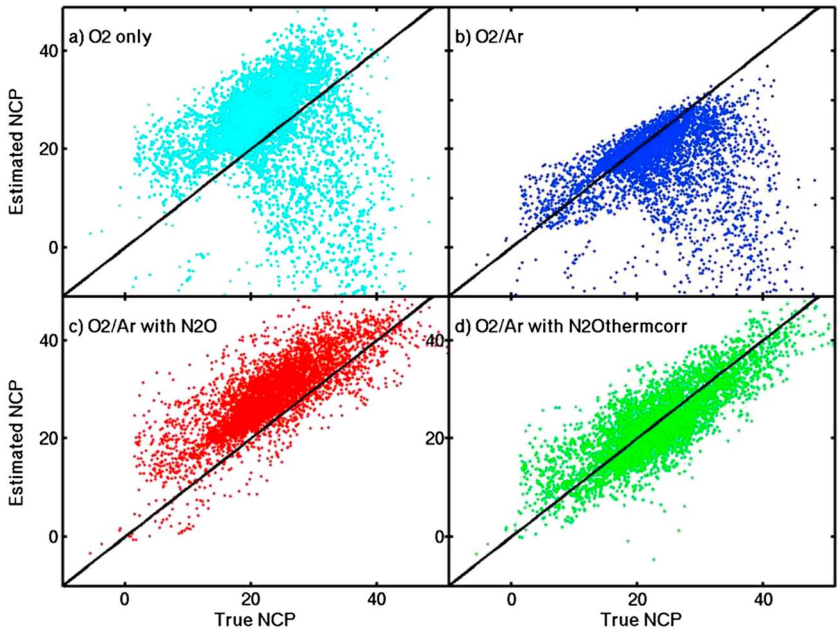

Figure 3. Comparison of true NCP to estimated NCP (mmol C m^{-2} d^{-1}) based on O_2, O_2/Ar, O_2/Ar-N_2O, and O_2/Ar-$N_2O_{thermcorr}$ gas fluxes for October to March in the region between 41°S and 60°S. Black lines represent the identity (1:1) slope. See caption of Figure 2 for description of equations.

3.3. Caveats and Limitations

The method relies on a strong stoichiometric relationship between O_2 and N_2O at depth. This is generally applicable in the Southern Ocean, where the euphotic zone is of similar depth to the mixed layer during the growing season, and waters at depth are oxic. In regions where the euphotic depth extends beyond the mixed layer depth (e.g., oligotrophic regions) and in oxygen minimum zones where denitrification is also an important contributor to N_2O cycling (e.g., Eastern Equatorial Pacific), the N_2O-based correction of the biological oxygen flux may not be suitable. In addition, the equations above do not account for potential N_2O production due to ammonia oxidation in the euphotic zone [e.g., *Dore and Karl*, 1996; *Santoro et al*., 2011; *Smith et al*., 2014; *Yool et al*., 2007; *Zamora and Oschlies*, 2014]. Although most studies to date have assumed that such production is relatively small [*Rees et al*., 2011; *Kock et al*., 2012], in regions where it occurs, our method would tend to overestimate the N_2O correction and therefore NCP. Our method also neglects potential variations in background atmospheric N_2O over the oceans, although these are relatively small [e.g., *Rhee et al*., 2009] and can be partially accounted for with concurrent atmospheric measurements. Regardless, the N_2O tracer will have to be interpreted with caution under such circumstances.

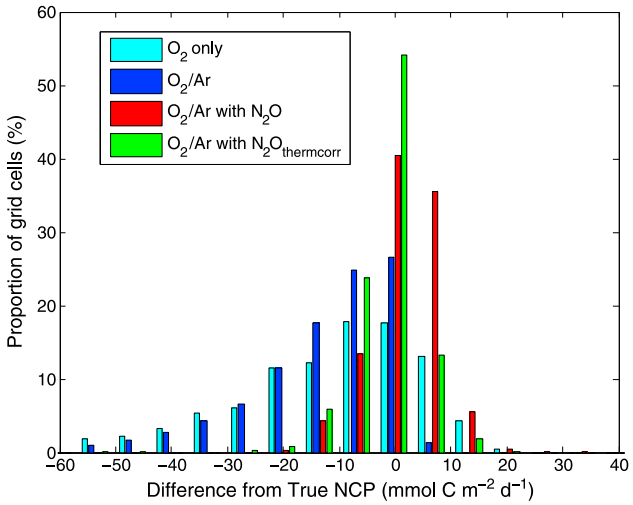

Figure 4. Frequency distribution of the difference between true and estimated NCP (mmol C m^{-2} d^{-1}) for the months of October and November between 41°S and 60°S. See caption of Figure 2 for description of equations.

A likely more important limitation on our method involves the uncertainty in the thermal N_2O component and our ability to measure it in the field. The equations above describe a correction based on biological N_2O, while underway measurements provide a measure of total N_2O, which is the sum of biological and physical components.

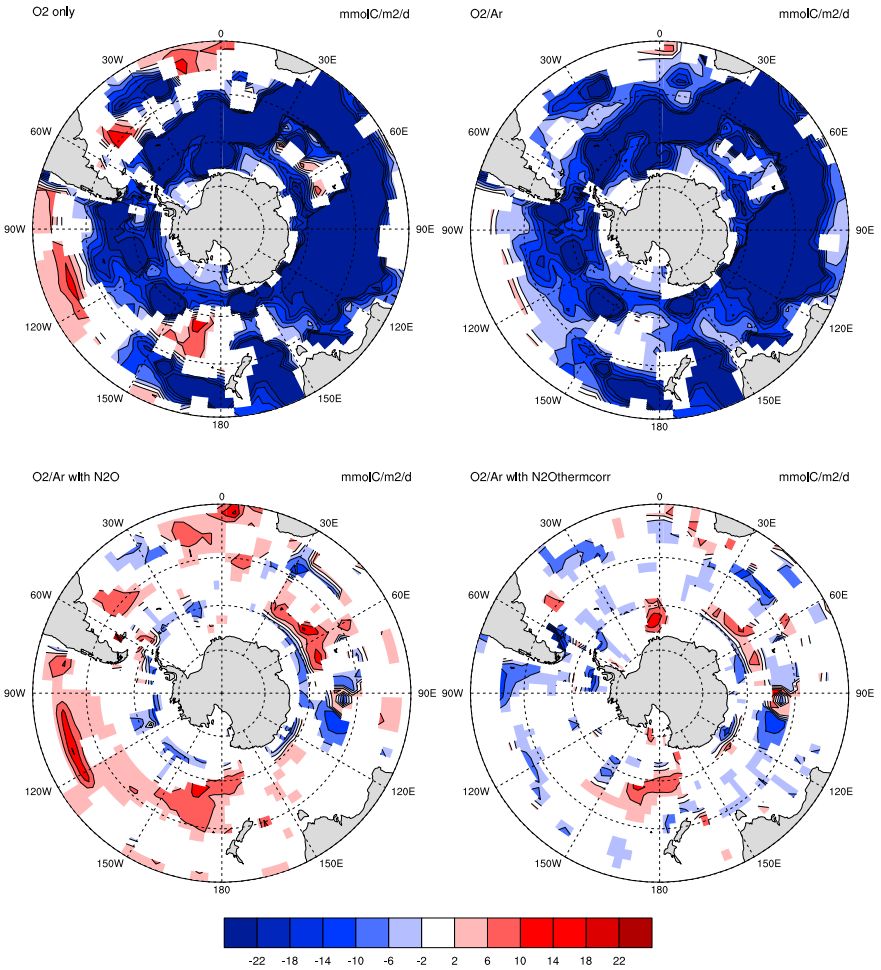

Figure 5. Stereographic map of the difference between true and estimated NCP based on O_2, O_2/Ar, O_2/Ar-N_2O, and O_2/Ar-$N_2O_{thermcorr}$ gas fluxes for the month of October (in mmol C m^{-2} d^{-1}). Deviations smaller than ±2 mmol C m^{-2} d^{-1} have been blanked out to better visualize the differences between the various approaches. See caption of Figure 2 for description of equations used.

Whereas O_2/Ar saturation is for all intents and purposes insensitive to physical processes by design, N_2O solubility is a function of physical processes including changes in temperature and salinity over the residence time of N_2O at the ocean surface (Figure 1 lower panel). Rapid cooling(warming) of surface waters with limited gas exchange can potentially lead to N_2O under(over)saturation, which will lead to an under(over)estimation of the vertical mixing component if estimates are based on total N_2O observations. For example, cooling of upper Circumpolar Deep Waters (uCDW) as they ventilate to the surface may lead to undersaturation if cooling occurs on faster timescales than equilibration with the atmosphere. Conversely, in the spring, warming of surface waters faster than gas equilibration kinetics can lead to thermal supersaturation in N_2O. This is likely the reason for the overestimation of NCP based on the total N_2O proxy in some regions of the Southern Ocean (Figure 3C).

The proportion of biological N_2O at the ocean surface can potentially be estimated as the residual of total observed N_2O minus a thermal component derived from satellite-based estimates of the oceanic heat flux over the residence time of N_2O in the mixed layer prior to the ship's presence. This estimate involves the following modification to equation (7),

$$NCP = k_{O2}\left(O_{2_{MLD}} - O_{2_{sat}}\right) - \frac{O_{2_{sat}}}{\mathrm{Ar}_{sat}} k_{Ar}\left(\mathrm{Ar}_{MLD} - \mathrm{Ar}_{sat}\right) - \frac{\partial O_{2_B}}{\partial (N_2O)_B} k_{N2O}\left([N_2O]_{Total} - [N_2O]_{Thermal} - [N_2O]_{sat}\right) \quad (8)$$

The thermal N_2O flux ($F_{N2OThermal}$) can be estimated with the following equation [*Keeling and Shertz*, 1992]:

$$F_{N2OThermal} = -\frac{d\left([N_2O]_{sat}\right)}{dT} * \frac{Q}{C_p} \quad (9)$$

where $\frac{d\left([N_2O]_{sat}\right)}{dT}$ is the temperature derivative of the N_2O solubility, and Q and C_p are the heat flux and ocean heat capacity, respectively. Because of the difference in air-sea exchange kinetics for heat and gases, the heat-flux correction will tend to overestimate $F_{N2OThermal}$. An "ad hoc" correction such as the one proposed by *Jin et al*. [2007] could be applied whereby the gas flux is reduced and delayed. The heat flux history can be estimated from satellite remote sensing and atmospheric model reanalyses [*Fairall et al*., 2003; *Yu and Weller*, 2007]. Such estimates have errors in the range of 5–15% [*Yu et al*., 2007], in par with errors associated with the windspeed gas exchange parameterization. Inserting equation (9) into equation (8), and rearranging:

$$NCP = k_{O2}\left(O_{2MLD} - O_{2sat}\right) - \frac{O_{2sat}}{\mathrm{Ar}_{sat}} k_{Ar}\left(\mathrm{Ar}_{MLD} - \mathrm{Ar}_{sat}\right) - \frac{\partial O_{2_B}}{\partial (N_2O)_B} k_{N2O}\left([N_2O]_{Total} - [N_2O]_{sat}\right)$$
$$- \frac{\partial O_{2_B}}{\partial (N_2O)_B}\left(\frac{d\left([N_2O]_{sat}\right)}{dT} * \frac{Q}{C_p}\right) \quad (10)$$

In other words, NCP can be estimated from the O_2, Ar, and N_2O fluxes, accounting for the effect of heat fluxes on the latter term. In reality, it is difficult to estimate $(N_2O)_B$ at depth because there are no heat flux estimates equivalent to satellite estimates. For this reason, we use the ratio $\frac{\partial O_{2_B}}{\partial N_2O}$ in our model calculations because it can be measured at sea. We find that the approximation is good enough, even when accounting for measurement uncertainties (see supporting information), to represent a significant improvement over the O_2/Ar-only, and the total N_2O correction for that matter (Figure 4). At the very least, such an approach provides a qualitative way to estimate where the N_2O signal may have a strong thermal component, and where a correction for vertical mixing should be interpreted with caution. Regardless, our study shows that N_2O (total, or corrected for the thermal component) measurements provide an improvement compared to O_2/Ar-only measurements (Figure 4). Overall, our proof-of-concept study demonstrates the potential improvement in NCP estimates associated with including N_2O observations and suggests the value of conducting field studies to ground proof the model results presented here.

Acknowledgments

A portion of this paper was written while NC was on sabbatical leave at Caltech and Université Pierre-et-Marie Curie (Sorbonne University). NC would like to thank his hosts for support and hospitality. NC was partly funded by an Alfred P. Sloan fellowship. Model results are available upon request from the corresponding author. The authors thank two anonymous reviewers for valuable comments.

Peter Strutton thanks two anonymous reviewers for their assistance in evaluating this paper.

References

Arévalo-Martínez, D. L., M. Beyer, M. Krumbholz, I. Piller, A. Kock, T. Steinhoff, A. Körtzinger, and H. W. Bange (2013), A new method for continuous measurements of oceanic and atmospheric N_2O, CO and CO_2: Performance of off-axis integrated cavity output spectroscopy (OA-ICOS) coupled to non-dispersive infrared detection (NDIR), *Ocean Sci.*, *9*(6), 1071–1087.

Bange, H. W., and M. O. Andreae (1999), Nitrous oxide in the deep waters of the world's oceans, *Global Biogeochem. Cycles*, *13*(4), 1127–1135, doi:10.1029/1999GB900082.

Bender, M. L., S. Kinter, N. Cassar, and R. Wanninkhof (2011), Evaluating gas transfer velocity parameterizations using upper ocean radon distributions, *J. Geophys. Res.*, *116*, C02010, doi:10.1029/2009JC005805.

Boontanon, N., S. Watanabe, T. Odate, and N. Yoshida (2010), Production and consumption mechanisms of N_2O in the Southern Ocean revealed from its isotopomer ratios, *Biogeosci. Discuss.*, *7*(5), 7821–7848.

Cassar, N., M. L. Bender, B. A. Barnett, S. Fan, W. J. Moxim, H. Levy, and B. Tilbrook (2007), The Southern Ocean biological response to aeolian iron deposition, *Science*, *317*(5841), 1067–1070.

Cassar, N., B. A. Barnett, M. L. Bender, J. Kaiser, R. C. Hamme, and B. Tilbrook (2009), Continuous High-Frequency Dissolved O_2/Ar Measurements by Equilibrator Inlet Mass Spectrometry, *Anal. Chem.*, *81*(5), 1855–1864.

Cassar, N., P. J. DiFiore, B. A. Barnett, M. L. Bender, A. R. Bowie, B. Tilbrook, K. Petrou, K. J. Westwood, S. W. Wright, and D. Lefevre (2011), The influence of iron and light on net community production in the Subantarctic and Polar Frontal Zones, *Biogeosciences*, *8*(2), 227–237.

Castro-Morales, K., N. Cassar, D. R. Shoosmith, and J. Kaiser (2013), Biological production in the Bellingshausen Sea from oxygen-to-argon ratios and oxygen triple isotopes, *Biogeosciences*, *10*(4), 2273–2291.

Cohen, Y., and L. I. Gordon (1978), Nitrous-oxide in oxygen minimum of Eastern Tropical North Pacific - Evidence for its consumption during denitrification and possible mechanisms for its production, *Deep Sea Res.*, *25*(6), 509–524.

Cohen, Y., and L. I. Gordon (1979), Nitrous oxide production in the Ocean, *J. Geophys. Res.*, *84*(Nc1), 347–353, doi:10.1029/JC084iC01p00347.

Craig, H., and T. Hayward (1987), Oxygen supersaturation in the ocean - biological versus physical contributions, *Science*, *235*(4785), 199–202.

Dore, J. E., and D. M. Karl (1996), Nitrification in the euphotic zone as a source for nitrite, nitrate, and nitrous oxide at Station ALOHA, *Limnol. Oceanogr.*, *41*(8), 1619–1628.

Duarte, C. M., A. Regaudie-de-Gioux, J. M. Arrieta, A. Delgado-Huertas, and S. Agusti (2013), The oligotrophic ocean is heterotrophic, *Annu. Rev. Mar. Sci.*, *5*(5), 551–569.

Ducklow, H. W., and S. C. Doney (2013), What is the metabolic state of the oligotrophic ocean? A debate, *Annu. Rev. Mar. Sci.*, *5*(5), 525–533.

Dutkiewicz, S., M. J. Follows, and P. Parekh (2005), Interactions of the iron and phosphorus cycles: A three-dimensional model study, *Global Biogeochem. Cycles*, *19*, GB1021, doi:10.1029/2004GB002342.

Elkins, J. W., S. C. Wofsy, M. B. Mcelroy, C. E. Kolb, and W. A. Kaplan (1978), Aquatic Sources and Sinks for Nitrous-Oxide, *Nature*, *275*(5681), 602–606.

Fairall, C. W., E. F. Bradley, J. E. Hare, A. A. Grachev, and J. B. Edson (2003), Bulk parameterization of air-sea fluxes: Updates and verification for the COARE algorithm, *J. Clim.*, *16*(4), 571–591.
Gent, P. R., and J. C. Mcwilliams (1990), Isopycnal mixing in ocean circulation models, *J. Phys. Oceanogr.*, *20*(1), 150–155.
Giesbrecht, K. E., R. C. Hamme, and S. R. Emerson (2012), Biological productivity along Line P in the subarctic northeast Pacific: In situ versus incubation-based methods, *Global Biogeochem. Cycles*, *26*, GB3028, doi:10.1029/2012GB004349.
Grefe, I., and J. Kaiser (2013), Equilibrator-based measurements of dissolved nitrous oxide in the surface ocean using an integrated cavity output laser absorption spectrometer, *Ocean Sci. Discuss.*, *10*(4), 1031–1065.
Hamme, R. C., and J. P. Severinghaus (2007), Trace gas disequilibria during deep-water formation, *Deep Sea Res., Part I*, *54*(6), 939–950.
Hamme, R. C., et al. (2012), Dissolved O_2/Ar and other methods reveal rapid changes in productivity during a Lagrangian experiment in the Southern Ocean, *J. Geophys. Res.*, *117*, C00F12, doi:10.1029/2011JC007046.
Hirsch, A. I., A. M. Michalak, L. M. Bruhwiler, W. Peters, E. J. Dlugokencky, and P. P. Tans (2006), Inverse modeling estimates of the global nitrous oxide surface flux from 1998-2001, *Global Biogeochem. Cycles*, *20*, GB1008, doi:10.1029/2004GB002443.
Horrigan, S. G., A. F. Carlucci, and P. M. Williams (1981), Light inhibition of nitrification in sea-surface films, *J. Mar. Res.*, *39*(3), 557–565.
Huang, K., H. Ducklow, M. Vernet, N. Cassar, and M. L. Bender (2012), Export production and its regulating factors in the West Antarctica Peninsula region of the Southern Ocean, *Global Biogeochem. Cycles*, *26*, GB2005, doi:10.1029/2010GB004028.
Jiang, S., P. H. Stone, and P. Malanotte-Rizzoli (1999), An assessment of the Geophysical Fluid Dynamics Laboratory ocean model with coarse resolution: Annual-mean climatology, *J. Geophys. Res.*, *104*(C11), 25,623–25,645, doi:10.1029/1999JC900095.
Jin, X., R. G. Najjar, F. Louanchi, and S. C. Doney (2007), A modeling study of the seasonal oxygen budget of the global ocean, *J. Geophys. Res.*, *112*, C05017, doi:10.1029/2006JC003731.
Jonsson, B. F., S. C. Doney, J. Dunne, and M. Bender (2013), Evaluation of the Southern Ocean O_2/Ar-based NCP estimates in a model framework, *J. Geophys. Res. Biogeosci.*, *118*, 385–399, doi:10.1002/Jgrg.20032.
Keeling, R. F., and S. R. Shertz (1992), Seasonal and interannual variations in atmospheric oxygen and implications for the global carbon-cycle, *Nature*, *358*(6389), 723–727.
Kock, A., J. Schafstall, M. Dengler, P. Brandt, and H. W. Bange (2012), Sea-to-air and diapycnal nitrous oxide fluxes in the eastern tropical North Atlantic Ocean, *Biogeosciences*, *9*(3), 957–964.
Law, C. S., and N. J. P. Owens (1990), Denitrification and nitrous-oxide in the North-Sea, *Neth. J. Sea Res.*, *25*(1-2), 65–74.
Laws, E. A. (1991), Photosynthetic quotients, new production and net community production in the open ocean, *Deep Sea Res., Part I*, *38*(1A), 143–167.
Lenton, A., et al. (2013), Sea-air CO_2 fluxes in the Southern Ocean for the period 1990-2009, *Biogeosciences*, *10*(6), 4037–4054.
Lueker, T. J., S. J. Walker, M. K. Vollmer, R. F. Keeling, C. D. Nevison, R. F. Weiss, and H. E. Garcia (2003), Coastal upwelling air-sea fluxes revealed in atmospheric observations of O-2/N-2, CO_2 and N_2O, *Geophys. Res. Lett.*, *30*(6), 1292, doi:10.1029/2002GL016615.
Manizza, M., R. F. Keeling, and C. D. Nevison (2012), On the processes controlling the seasonal cycles of the air-sea fluxes of O_2 and N_2O: A modelling study, *Tellus B*, *64*, 18429, doi:10.3402/tellusb.v64i0.18429.
Marshall, J., C. Hill, L. Perelman, and A. Adcroft (1997), Hydrostatic, quasi-hydrostatic, and nonhydrostatic ocean modeling, *J. Geophys. Res.*, *102*(C3), 5733–5752, doi:10.1029/96JC02776.
Martin, P., et al. (2013), Iron fertilization enhanced net community production but not downward particle flux during the Southern Ocean iron fertilization experiment LOHAFEX, *Global Biogeochem. Cycles*, *27*, 871–881, doi:10.1002/gbc.20077.
Nevison, C. D., R. F. Weiss, and D. J. Erickson (1995), Global Oceanic Emissions of Nitrous-Oxide, *J. Geophys. Res.*, *100*(C8), 15,809–15,820, doi:10.1029/95JC00684.
Nevison, C. D., J. H. Butler, and J. W. Elkins (2003), Global distribution of N_2O and the DELTA N_2O-AOU yield in the subsurface ocean, *Global Biogeochem. Cycles*, *17*(4), 1119, doi:10.1029/2003GB002068.
Nevison, C. D., R. F. Keeling, R. F. Weiss, B. N. Popp, X. Jin, P. J. Fraser, L. W. Porter, and P. G. Hess (2005), Southern Ocean ventilation inferred from seasonal cycles of atmospheric N_2O and O_2/N_2 at Cape Grim, Tasmania, *Tellus B*, *57*(3), 218–229.
Nevison, C. D., R. F. Keeling, M. Kahru, M. Manizza, B. G. Mitchell, and N. Cassar (2012), Estimating net community production in the Southern Ocean based on atmospheric potential oxygen and satellite ocean color data, *Global Biogeochem. Cycles*, *26*, GB1020, doi:10.1029/2011GB004040.
Nicholson, D., R. H. R. Stanley, and S. C. Doney (2014), The triple oxygen isotope tracer of primary productivity in a dynamic ocean model, *Global Biogeochem. Cycles*, *28*, 538–552, doi:10.1002/2013GB004704.
Oudot, C., C. Andrie, and Y. Montel (1990), Nitrous-Oxide Production in the Tropical Atlantic-Ocean, *Deep Sea Res., Part I*, *37*(2), 183–202.
Palevsky, H. I., F. Ribalet, J. E. Swalwell, C. E. Cosca, E. D. Cokelet, R. A. Feely, E. V. Armbrust, and P. D. Quay (2013), The influence of net community production and phytoplankton community structure on CO_2 uptake in the Gulf of Alaska, *Global Biogeochem. Cycles*, *27*, 664–676, doi:10.1002/gbc.20058.
Peng, T. H., W. S. Broecker, G. G. Mathieu, and Y. H. Li (1979), Radon Evasion Rates in the Atlantic and Pacific Oceans as Determined during the Geosecs Program, *J. Geophys. Res.*, *84*(Nc5), 2471–2486, doi:10.1029/JC084iC05p02471.
Rees, A. P., N. J. P. Owens, and R. C. UpstillGoddard (1997), Nitrous oxide in the Bellingshausen Sea and Drake Passage, *J. Geophys. Res.*, *102*(C2), 3383–3391, doi:10.1029/96JC03350.
Rees, A. P., I. J. Brown, D. R. Clark, and R. Torres (2011), The Lagrangian progression of nitrous oxide within filaments formed in the Mauritanian upwelling, *Geophys Res Lett*, *38*, L21606, doi:10.1029/2011GL049322.
Reuer, M. K., B. A. Barnett, M. L. Bender, P. G. Falkowski, and M. B. Hendricks (2007), New estimates of Southern Ocean biological production rates from O_2/Ar Ratios and the triple isotope composition of O_2, *Deep Sea Res., Part I*, *54*, 951–974.
Rhee, T. S., A. J. Kettle, and M. O. Andreae (2009), Methane and nitrous oxide emissions from the ocean: A reassessment using basin-wide observations in the Atlantic, *J. Geophys. Res.*, *114*, D12304, doi:10.1029/2008JD011662.
Rodgers, K. B., O. Aumont, S. E. Mikaloff Fletcher, Y. Plancherel, L. Bopp, C. de Boyer Montégut, D. Iudicone, R. F. Keeling, G. Madec, and R. Wanninkhof (2014), Strong sensitivity of Southern Ocean carbon uptake and nutrient cycling to wind stirring, *Biogeosciences*, *11*(15), 4077–4098.
Saikawa, E., et al. (2014), Global and regional emissions estimates for N_2O, *Atmos. Chem. Phys.*, *14*(9), 4617–4641.
Santoro, A. E., C. Buchwald, M. R. McIlvin, and K. L. Casciotti (2011), Isotopic Signature of N_2O Produced by Marine Ammonia-Oxidizing Archaea, *Science*, *333*(6047), 1282–1285.
Seitzinger, S. P., C. Kroeze, and R. V. Styles (2000), Global distribution of N_2O emissions from aquatic systems: Natural emissions and anthropogenic effects, *Chemosphere: Global Change Sci.*, *2*(3–4), 267–279.
Smith, J. M., K. L. Casciotti, F. P. Chavez, and C. A. Francis (2014), Differential contributions of archaeal ammonia oxidizer ecotypes to nitrification in coastal surface waters, *ISME J.*, *8*(8), 1704–1714.

Spitzer, W. S., and W. J. Jenkins (1989), Rates of vertical mixing, gas-exchange and new production - estimates from seasonal gas cycles in the upper ocean near Bermuda, *J. Mar. Res.*, *47*(1), 169–196.

Stanley, R. H. R., J. B. Kirkpatrick, N. Cassar, B. A. Barnett, and M. L. Bender (2010), Net community production and gross primary production rates in the western equatorial Pacific, *Global Biogeochem. Cycles*, *24*, GB4001, doi:10.1029/2009GB003651.

Stephens, B. B., R. F. Keeling, M. Heimann, K. D. Six, R. Murnane, and K. Caldeira (1998), Testing global ocean carbon cycle models using measurements of atmospheric O_2 and CO_2 concentration, *Global Biogeochem. Cycles*, *12*(2), 213–230, doi:10.1029/97GB03500.

Suntharalingam, P., and J. L. Sarmiento (2000), Factors governing the oceanic nitrous oxide distribution: Simulations with an ocean general circulation model, *Global Biogeochem. Cycles*, *14*(1), 429–454, doi:10.1029/1999GB900032.

Thompson, R. L., et al. (2014), Nitrous oxide emissions 1999 to 2009 from a global atmospheric inversion, *Atmos. Chem. Phys.*, *14*(4), 1801–1817.

Tortell, P. (2005), Dissolved gas measurements in oceanic waters made by membrane inlet mass spectrometry, *Limnol. Oceanogr. Methods*, *3*, 24–37.

Trenberth, K. E., J. G. Olson, and W. G. Large (1989), A Global Ocean Wind Stress Climatology Based on ECMWF Analyses, Tech. Rep. NCAR/TN-338+STR, National Center for Atmospheric Research, Boulder, Colo.

van der Loeff, M. M. R., N. Cassar, M. Nicolaus, B. Rabe, and I. Stimac (2014), The influence of sea ice cover on air-sea gas exchange estimated with radon-222 profiles, *J. Geophys. Res. Oceans*, *119*, 2735–2751, doi:2710.1002/2013JC009321.

Walter, S., H. W. Bange, U. Breitenbach, and D. W. R. Wallace (2006), Nitrous oxide in the North Atlantic Ocean, *Biogeosciences*, *3*(4), 607–619.

Wanninkhof, R. (1992), Relationship between wind speed and gas exchange over the ocean, *J. Geophys. Res.*, *97*(C5), 7373–7382, doi:10.1029/92JC00188.

Weeding, B., and T. W. Trull (2014), Hourly oxygen and total gas tension measurements at the Southern Ocean Time Series site reveal winter ventilation and spring net community production, *J. Geophys. Res. Oceans*, *119*, 348–358.

Williams, P. J. L., P. D. Quay, T. K. Westberry, and M. J. Behrenfeld (2013), The oligotrophic ocean is autotrophic, *Annu. Rev. Mar. Sci.*, *5*(5), 535–549.

Yool, A., A. P. Martin, C. Fernandez, and D. R. Clark (2007), The significance of nitrification for oceanic new production, *Nature*, *447*(7147), 999–1002.

Yoshinari, T. (1976), Nitrous oxide in the sea, *Mar. Chem.*, *4*(2), 189–202.

Yu, L. S., and R. A. Weller (2007), Objectively analyzed air-sea heat fluxes for the global ice-free oceans (1981-2005), *Bull. Am. Meteorol. Soc.*, *88*(*4*), 527–539.

Yu, L. S., X. Z. Jin, and R. A. Weller (2007), Annual, seasonal, and interannual variability of air-sea heat fluxes in the Indian Ocean, *J. Clim.*, *20*(13), 3190–3209.

Zamora, L. M., and A. Oschlies (2014), Surface nitrification: A major uncertainty in marine N_2O emissions, *Geophys. Res. Lett.*, *41*, 4247–4253, doi:10.1002/2014GL060556.